

Quantum transistors for heat flux in and out of working substance parts: harmonic vs transmon and Kerr environs

Deepika Bhargava^{1,2}, Paranjay Chaki², Aparajita Bhattacharyya², Ujjwal Sen²

¹Indian Institute of Science Education and Research, Homi Bhabha Rd, Pashan, Pune 411 008, India and

²Harish-Chandra Research Institute, A CI of Homi Bhabha National Institute, Chhatnag Road, Jhunsi, Prayagraj 211 019, India

Quantum thermal transistors have been widely studied in the context of three-qubit systems, where each qubit interacts separately with a Markovian harmonic bath. Markovianity is an assumption that is imposed on a system if the environment loses its memory within short while, while non-Markovianity is a general feature, inherently present in a large fraction of realistic scenarios. Instead of Markovian environments, here we propose a transistor in which the interaction between the working substance and an environment comprising of an infinite chain of qutrits is based on periodic collisions. We refer to the device as a working-substance thermal transistor, since the model focuses on heat currents flowing in and out of each individual qubit of the working substance to and from different parts of the system and environment. We find that the transistor effect prevails in this apparatus and we depict how the amplification of heat currents depends on the temperature of the modulating environment, the system-environment coupling strength and the interaction time. Initially we consider no direct coupling between the left and right qubits, and only the left-middle and right-middle terminals are coupled. Later, we also investigate both symmetric and asymmetric coupling configurations where the left and right qubits are coupled to each other, and observe amplification in the left and right qubits in both the cases. We further show that there exists a non-zero amplification even if one of the environments, that is not the modulating one, is detached from the system. Additionally, the environment, being comprised of three-level systems, allows us to consider the effects of frail perturbations in the energy-spacings of the qutrit, leading to a non-linearity in the environment. We consider non-linearities that are either of transmon- or of Kerr-type. We find parameter ranges where there is a significant amplification for both transmon- and Kerr-type non-linearities in the environment. The analysis is performed under the condition of vanishing left-right coupling, along with the symmetric and asymmetric coupling configurations as well. Furthermore, we demonstrate a prominent transistor effect for the working substance when coupled to qubit environments, within the same collisional model framework. Finally, we detect the non-Markovianity induced in the system from a non-monotonic behavior of the amplification observed with respect to time, and quantify it using the distinguishability-based measure of non-Markovianity, for all the three cases mentioned above.

I. INTRODUCTION

Advancements in science and technology have led to the development of modern equipment that requires miniaturized electrical circuits. These small-scale components exhibit thermal and quantum properties that impact performance of the device, making control over electrical and thermal fluctuations crucial. A transistor is a device that controls current flow in electric circuits [1–4]. Electrical transistors are essential for modern technology, utilized in amplifiers, switches, and transformers. Since their invention by Bardeen and Brattain [1], extensive research has focused on improving and adapting transistor-based devices [2–7].

A quantum thermal transistor (QTT) [8] is the quantum analog of an electric transistor, used to control heat currents in miniaturized circuits. Quantum effects enable operations not possible in classical systems, offering advantages over traditional devices. Other quantum thermal machines like quantum batteries [9–11], quantum refrigerators [12–14], quantum thermal diodes [15], and quantum rectifiers [16–18] have been devised which exploit quantum mechanical properties of the system. Since the introduction of the quantum thermal transistor by Joulain et al. in 2016 [8], significant progress has been made, particularly in systems involving Markovian environments [19–25].

Current QTT models typically utilize a three-qubit working substance, each connected to a Markovian bath. Other models include qubit-qutrit systems [26] and those employ-

ing periodic control, such as the Floquet quantum thermal transistor [27, 28]. There are extensive works which consider Coulomb-coupled conductors [29, 30], polarons in the context of non-equilibrium systems [31], double cavity optomechanical systems [32], and three terminal normal-superconductors [33] as models for QTTs. QTT performance, including environmental effects with and without noise, has been extensively studied in single and multi-transistor systems with shared baths. [34–37]. The significance of quantum coherence in the context of QTT has also been studied, which enables to provide quantum advantage in the amplification of a QTT over its classical counterpart [38]. Further studies on QTT focus on negative differential thermal conductance (NDTC) for high amplification rates and the role of strong coupling and quantum coherence in achieving NDTC [39–42]. Models analogous to these classical ones, but employing QTTs, have also been rigorously investigated. In particular, configurations such as the Darlington setup [43, 44], where the output of one transistor serves as the input to another, or more complex transistor networks as considered in [45], have been shown to provide significant performance enhancements compared to scenarios that do not incorporate QTTs. Experimental realization of QTTs using superconducting circuits [46, 47], materials like VO_2 [48, 49], and implementation using magnetic thermal transistor [50] have been carried out.

Previous QTT studies utilize a global heat current approach, treating the system as three qubits where the focus is on the

heat flowing from each bath into the entire working substance. The heat current is "global" in a sense that the heat current corresponding to each of the baths flow globally into the entire working substance. This paper focuses on local heat currents, where we concentrate on the heat currents flowing "locally" into each qubit from different parts of the system and environment, in contrast to the global heat current approach. We have considered this approach since we know the characteristics of the sub-parts of the working substance experimentally, and it is essential to control and regulate the heat flow in the sub-parts of the system in order to preserve the material for actual implementations in circuits. Our concept of such local heat current is novel, and is hitherto unexplored in literature. There have been previous works which discuss the different types of heat currents in thermal equilibrium [51], where the system is connected to an Ohmic bath with a given spectral density. Here, they have used certain approximations to derive the local master equation and subsequently the definition of the local heat current. These assumptions are as follows. Firstly, the interaction between system and environment is perturbatively very small. Secondly, the Markov approximation assumption is made which tells about the invariance of system's state on time scales of order correlation time. However, these assumptions are not valid in our case. We have defined our system for arbitrary coupling instead of weak coupling which does not follow the Born approximation. The Markov approximation also talks about the bath retaining its state during and after the evolution, which is not true in the dynamics we have considered. Our definition of a local heat current is not equivalent to their definition since the Born Markov assumptions on which they have defined the local heat current are not valid in our system.

In our case, the working substance is considered under the most general completely positive trace-preserving (CPTP) dynamics, i.e. its evolution is described by a global unitary acting on the joint system of the working substance and its environment, followed by discarding the environment. Importantly, no assumption of Markovianity is made in the analysis, and therefore, Markovian master equations do not naturally arise in this framework.

In Ref. [52], for instance, it has been rigorously proven how local master equations are consistent with the laws of thermodynamics. As Markovian nature of a thermal environment, in general, arises under some specific assumptions, and is very unlikely to obtain in a practical scenario, it is important to study the effect of non-Markovianity on transistor action. Quantum thermal devices in the context of non-Markovian environments have been previously delved into [53–56], which mainly focused on spin-environments. However, here we consider the system-environment interaction to be modeled by a collisional model comprising an infinite array of qutrits, which is experimentally feasible to implement and is fundamentally different from the Markovian environment scenario.

We provide a prototype of a QTT, which consists of three qubits interacting with each other and each qubit is connected separately to an environment. The interaction between the system and environment mimics the collisional model [57–61], which has been extensively studied in literature in the

context of quantum batteries [62, 63], equilibrium and non-equilibrium dynamics [58–60, 64, 65], strong coupling thermodynamics [66] and the impact of quantum coherence in thermodynamics [67, 68]. In the model that we consider, each system qubit sequentially interacts with a qutrit of the environment for a short but fixed duration of time. The environment, which originally consists of infinite number three-level systems with equispaced energy levels, also allows us to consider the effects of frail perturbations in the energies of the environment-particles, leading to unequal energy spacings of each qutrit. Considering this model as the environment instead of the usual Markovian bosonic one, introduces an inherent non-Markovianity in the system. Using this model, we devise our transistor, which can control and regulate heat currents in the sub-parts of the working substance.

In this work, we scrutinize a class of transistors comprising a three-qubit working substance which interacts with the environment via the collisional model. There also exist interactions between the components of the working substance, i.e. the left, middle, and right qubits. Initially, we consider equal interaction strength between the left-middle and right-middle qubits, but the left and right qubits remain non-interacting. We find significant amplification of the heat currents at two terminals of the transistor, being modulated by the heat current at the remaining terminal. The amplification factor depends on the temperature of the modulating environment, and system-environment coupling. Specifically, the amplification factors for the left and right qubits first increase and then decrease, as the modulating temperature rises. The amplification trend with coupling strength is complex: it decreases below a critical temperature but increases beyond it with stronger interactions. We also observe some amplification with fewer than three local environments. Additionally, in a linear system with equispaced energy levels, external perturbations can induce small fluctuations, effectively rendering the system nonlinear. Two examples of where such a situation naturally arises are transmons [69–73] and Kerr-type environments [74]. In our work, apart from considering non-Markovian environment, which constitutes the collisional model of qubits interacting sequentially with equispaced qutrits, we also consider the effects of non-linearities in the environment such as in transmon and Kerr-types, in the amplification of a type of transistor. We find that amplification and its temperature dependence persist even with small non-linearities in the qutrit energy levels. Transmon and Kerr-type non-linearities enhance amplification in different temperature regimes. Below a critical temperature, Kerr non-linearities outperform linear qutrits, while above it, transmon qutrits are more effective. Furthermore, we find a non-monotonic behavior in the amplification factor of the three-qubit transistor setup with respect to time, and quantify the non-Markovianity that possibly induces such behavior. Furthermore, we consider two cases, i.e. symmetric and asymmetric coupling, where for symmetric coupling, left-middle, middle-left, and left-right qubits of working substance are coupled with each other by equal interaction strength. On the other hand, for asymmetric coupling, left-middle, middle-left, and left-right qubits are coupled by different interaction strengths. We show that appreciable amplification is obtain-

able for both the cases corresponding to both left and right qubits. Moreover, we also observe the benefits of nonlinear environments in obtaining higher amplification in both symmetric and asymmetric cases. Finally, instead of considering the environment to be a collision model composed of qutrits, we consider the collision model to consist of a qubit system and again show sufficient amplification corresponding to both right and left qubits. Moreover, we analyze the effects of nonlinearities present in the environment in this setting. We scrutinize the distance-based non-Markovianity measure in this situation as well.

The paper is organized as follows. In Sec. II, we explicitly describe the collisional model for the system and environment that we consider, along with defining the relevant Hamiltonians, the dynamical amplification factor, and the different types of heat-currents. We then analyze the effect of varying temperature of the modulating bath, and coupling constant between the bath and the working substance on the amplification, along with the symmetric and asymmetric cases, considering linear baths in Sec. III. We consider both the cases where there are three (Sec. III A) and less than three (Sec. III B) environments. We then introduce non-linearity in the baths and analyze its effect on amplification in Sec. IV. In Sec. V, the non-Markovianity present in the system is quantified and analyzed. Analysis of the transistor effect using qubits as components of the environment is provided in Sec. VI. Finally the concluding remarks are presented in Sec. VII.

II. WORKING-SUBSTANCE THERMAL TRANSISTOR

An electrical transistor is a three terminal device which consists of a p-type (n-type) semiconductor sandwiched between two n-type (p-type) semiconductors to form a n-p-n (p-n-p) junction. The three terminals, corresponding to n-p-n, are often referred to as emitter, base and collector, and the currents flowing into each of these terminals are the emitter, base and collector currents, denoted by I_E , I_B and I_C respectively. The function of an electrical transistor is to amplify the input base current to the output collector current, while operating in the common emitter mode. The figure of merit that quantifies the performance of a transistor is given by the dimensionless quantity, direct current (DC) amplification factor, β_{DC} , which is defined as

$$\beta_{DC} = \frac{I_C}{I_B}.$$

This figure of merit is useful, particularly in transistor circuits where all the currents are constant with respect to time. Meanwhile, if the currents are functions of time, the alternating current (AC) amplification factor, β_{AC} , is defined as

$$\beta_{AC} = \frac{\Delta I_C}{\Delta I_B},$$

where ΔI_C and ΔI_B are the small changes in I_C and I_B in the AC circuit of the transistor. The amplification factor refers to the change in collector current due to a small change in base

current. Typically, the values of β_{DC} or β_{AC} is of the order of 200-300 and is an intrinsic property of an electrical transistor.

A QTT, on the other hand, is a thermal device which amplifies and modulates heat currents flowing into it, in analogy to an electrical transistor which amplifies electric currents. The quantum thermal transistor that we consider here consists of three two-level systems, which we refer to as the working substance. Each of these two-level systems is coupled separately to thermal environments. The interaction between the system and environment mimics that of the collisional model which we define in the succeeding subsection. We refer to the three two-level systems as L , M , and R which correspond to the left, middle, and right qubits, respectively. The energy differences between the two levels of the two-level systems are, respectively, given by $\hbar\omega_L$, $\hbar\omega_M$ and $\hbar\omega_R$. The temperatures of the three thermal environments attached to the qubits are T_L , T_M and T_R respectively. The middle environment is taken to be the modulating one which modulates the current in the left and right qubits analogous to its electrical counterpart. The dynamical amplification factor, α_X corresponding to the qubit- X , of a QTT is defined as

$$\alpha_X = \frac{\partial J_X}{\partial J_M} = \frac{\frac{\partial J_X}{\partial T_M}}{\frac{\partial J_M}{\partial T_M}} \quad (1)$$

where $X \in \{L, R\}$. The quantity, J_X , denotes the heat current flowing into the terminal X of the working substance. A more elaborate discussion on heat currents, focusing on the type of heat current that we consider, is explicitly provided in Sec. II C. The magnitude of amplification factor is indicative of how well the transistor performs, with the value of $|\alpha_X|$ being greater than 1 indicating that the transistor effect exists.

A. Collisional model for system-environment interaction: linear and non-linear

The transistor models, that have been hitherto explored, fundamentally constitute local Markovian environments connected to each qubit of a QTT, where the notion of heat current corresponding to the individual heat flow from each bath was relevant. Here we use a different approach to design a type of transistor model, and provide a somewhat distinct definition of heat current, where we look into the heat current flowing into each of the qubits separately. This is discussed in detail in subsection II C. Here we focus on the model of the environment that we consider. The working substance comprises three qubits, where each qubit is open to an environment. The environment constitutes an infinite number of three-level systems or qutrits. Each qutrit arrives one after the other, and interacts with a single qubit of the working substance for a fixed time, say δt . After each time interval, δt , a new qutrit pertaining to the environment arrives to interact with the qubit. Hence, the environment effectively resets after the finite interaction time, δt . Owing to the periodic collisions of the system with the environment, this model is often referred to in literature as the “collisional model” [57-61].

Initially we consider the energy difference between the ground and first excited states of each qutrit, that comprises

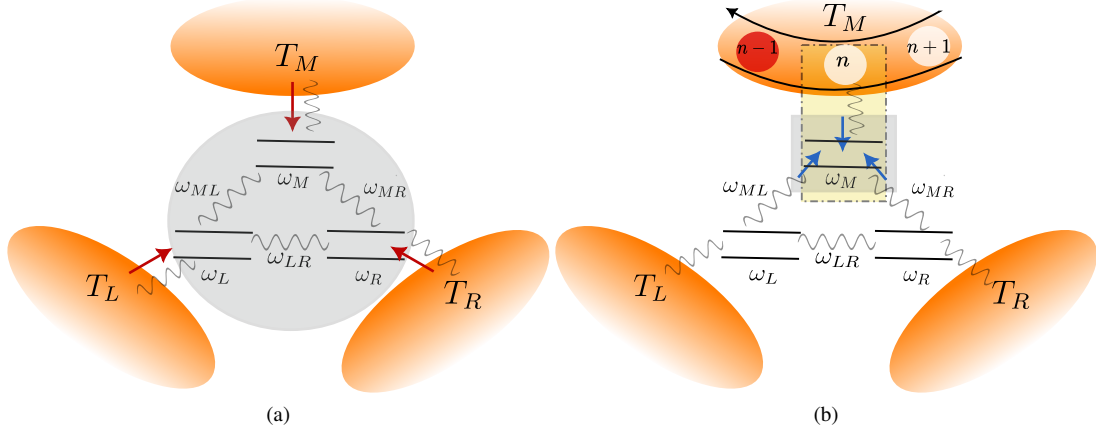


Figure 1. Schematic representation of the difference between the local and global approaches utilized to provide the definition of heat current used in previous models, referred to as BTTs versus the model studied in this paper, referred to as WTTs. The name, BTT essentially means that the transistor is conceptualized by looking at heat current flows in and out of each of the local baths to and from the entire system, as depicted by the red arrows in panel (a), and hence the transistor action is scrutinized by focusing on the “bath”. The name, WTT suggests that, the heat is exchanged between each (local) qubit with the different parts of the system and the environment, as shown by the blue arrows in panel (b), and therefore the focus is on the “working substance”. BTTs correspond to the usual QTT model previously studied in literature, while the class of transistor devices which we analyze in this paper are the WTTs. The bath interacts with the working substance via the collisional model where every qutrit sequentially interacts with the working substance. We show in the schematic that the n^{th} qubit is interacting with the system while the $(n-1)^{\text{th}}$ qubit has already interacted. The interaction with the $(n+1)^{\text{th}}$ qubit is going to occur.

the environment, to be equal to that between the first and second excited states of the qutrit. Since both the energy levels are equispaced, we refer to the type of environment comprising such qutrits to be a linear one. However in reality, there may be frail perturbations in the environment leading to small differences in the energy-level spacings. This introduces non-linearity in the environment due to a tweaking of the energy levels by a small amount. Let us say that the energy of the first excited level is increased by a small quantity. Then the energy gap between the ground state and the first excited state is greater than the difference between the first excited state and the second excited state. If the energy level differences decrease as we go to higher energy levels, then we get a transmon environment. Whereas if the energy level differences increase as we go from first to second excited states, a Kerr-type environment is generated. We refer to both these types of environments as non-linear ones.

B. Relevant Hamiltonians

In this subsection, we discuss the transistor model that we consider, including both the system and environment Hamiltonians, and the interactions between them. The Hamiltonian of the system comprising the three qubits is given by

$$H_{\text{sys}} = - \sum_{i \in \{L, M, R\}} \frac{\hbar \omega_i}{2} \sigma_z^i - \sum_{\substack{i, j \in \{L, M, R\} \\ i \neq j}} \frac{\hbar \omega_{ij}}{2} \sigma_z^i \sigma_z^j, \quad (2)$$

where σ_z refers to the Pauli- z matrix for spin-1/2 particles. Here L, M and R refers to the left, middle and right qubits

respectively. The first term represents the local Hamiltonian of each qubit, while the second term denotes the interaction between the qubits. The local Hamiltonian of a single qutrit of the environment is given by

$$H_{\text{env}} = -\hbar \Delta \sum_{i \in \{L, M, R\}} \sigma_z^{(i), \text{env}}, \quad (3)$$

where the energy levels of each qutrit are equispaced, and Δ is the energy gap between any two successive energy levels. Here $\sigma_z^{(i), \text{env}}$ is the Pauli- z matrix for spin-1 particles. The index i denotes the qutrit connected to i^{th} qubit of the system. The Pauli- x and Pauli- z matrices for spin-1 are respectively given by

$$\sigma_x^{\text{env}} = \frac{1}{\sqrt{2}} \begin{bmatrix} 0 & 1 & 0 \\ 1 & 0 & 1 \\ 0 & 1 & 0 \end{bmatrix}, \quad \sigma_z^{\text{env}} = \begin{bmatrix} 1 & 0 & 0 \\ 0 & 0 & 0 \\ 0 & 0 & -1 \end{bmatrix}.$$

In Sec. III, we consider the collisional model comprising of equispaced qutrits, which arrive one at a time to interact with the system qubit. Each of the three qubits interact locally with each qutrit of the environment via the qubit-qutrit interaction given by

$$H_{\text{qubit-env}} = -\hbar g \sum_{i \in \{L, M, R\}} \sigma_x^{(i), \text{qubit}} \sigma_x^{(i), \text{env}} \quad (4)$$

where $\sigma_x^{(i), \text{qubit}}$ is the Pauli- x matrix for spin-1/2 particle, $\sigma_x^{(i), \text{env}}$ is the Pauli- x matrix for spin-1 particle, and g

is the coupling constant between the system-qubit and the environment-qutrit. The quantities $\omega_i, \omega_{ij}, \Delta$ and g_k are all in units of time $^{-1}$, $\forall i, j$. For simplicity we consider $\omega_L = \omega_M = \omega_R = \omega_{ML} = \omega_{MR} = \Delta$ and $\omega_{LR} = 0$, unless stated otherwise.

The environment is modeled as an infinite sequence of three-level systems or qutrits, each of which sequentially interacts with a single qubit comprising the working substance. Each qutrit interacts with the qubit for a fixed duration δt , after which it is replaced by a new, identical qutrit. As a result, the environment effectively resets after each interaction interval δt . Due to this periodic interaction between the system and environmental units, this framework is commonly referred to in the literature as a collisional model. The dynamical nature of the environment - whether Markovian or non-Markovian - is determined by key parameters of the model, such as the coupling strength between the system and the environment and the collision time. If the interaction time between the system and each environmental qutrit is sufficiently small for a given interaction strength, the environment is able to extract information from the system but lacks the time necessary to return it. This results in Markovian dynamics, characterized by a lack of memory effects. Conversely, when the interaction time with each qutrit is increased, the environment can not only retain information about the system but also feed it back during subsequent interactions. This backflow of information leads to non-Markovian dynamics, wherein memory effects play a significant role. On the other hand, if the environmental qutrits interact perturbatively with the system, i.e., the interaction strength is very weak, and are subsequently replaced after each interaction, as prescribed by the collisional model, the environment fails to retain sufficient information to influence the evolution of the system. As a result, the system exhibits Markovian dynamics, characterized by the absence of memory effects. In contrast, when the system-environment interaction strength is increased, the environment becomes more entangled with the system and retains information about its past states. If the structure of subsequent interactions permits, this stored information can flow back into the system, thereby influencing its future dynamics and giving rise to non-Markovian behavior.

C. Relevant heat currents in working-substance thermal transistors

The performance of a QTT depends on how efficiently it can amplify the heat currents in the terminals, L and R , while being controlled by the flow of heat current at terminal M . The definition of heat current in the context of quantum transistors is given by the rate of change of energy of the working substance with respect to time, which focuses on the current flowing into and out of the individual baths. This scenario involves the consideration of local Markovian baths, where heat current is defined as

$$\mathcal{J}_X = \text{Tr}(H_{sys} \mathcal{L}_X[\rho]), X \in \{L, M, R\},$$

where ρ is the density matrix of the working substance, and $\mathcal{L}_X[\rho]$ is the Lindblad operator corresponding to the terminal X , that appears in the Gorini-Kossakolski-Sudarshan-Lindblad (GKSL) [75–77] master equation for the Markovian dynamics. We will refer to these transistors as bath thermal quantum transistors (BTTs) since in this case, one effectively considers the heat flowing in and out of a single bath into the entire working substance. This heat current is “global” in a sense that heat flows in and out of the entire system. We choose to focus on the heat current which flows in and out of each qubit of the working substance, to and from different parts of the system and environment, and refer to such type of transistors as working-substance thermal quantum transistors (WTTs) since the transistor action occurs due to the heat exchange between different parts of the system and environment, and a particular qubit. The local heat currents flowing in and out each X^{th} terminal of the working substance is defined by

$$J_X = \text{Tr}(\dot{\rho}_X H_X), \quad (5)$$

where $X \in \{L, M, R\}$. The operator, $\dot{\rho}_X$, denotes the rate of change of the reduced density matrix of the X^{th} terminal of the working substance. This type of heat current can be considered “local” in a sense that heat flows locally in and out of a particular subsystem of the working substance. The difference between the two approaches is pictorially depicted in Fig 1. This definition of heat current is constructed in a generalized setting, and is not derived via any master equation formalism.

In the fabrication of quantum devices, the material properties of the qubits, such as melting point, are typically well-characterized in advance and require minimal information about the surrounding environment. From this standpoint, analyzing heat currents from the perspective of the qubits themselves, rather than from the conventional bath-centric viewpoint, enables a direct correlation between these currents and the intrinsic material properties that are readily accessible in experiments. Such a system-focused definition of heat current has the potential to guide the design and optimization of qubit-based quantum devices whose performance is sensitive to the behavior of these currents.

In our work, the dynamics of the working substance is modeled as general CPTP dynamics, realized through global unitary evolution of the combined system and environment, followed by tracing out the environment. This framework goes beyond the Markovian assumption. Therefore our approach does not rely on master equations, neither global nor local and as the system does not relax to a steady state. Our numerical analysis further confirms that the system exhibits continuous time-dependent evolution without approaching a steady state. Consequently, since no steady state is attained, the currents do not sum to zero as in their classical counterparts. Within this setting, the definition of heat current that we introduce is novel, as it captures the flow of heat through the system even in the absence of a steady state.

To find the amplification factor, we calculate the first order partial derivatives numerically using the five-point formula. According to the five-point formula, the first order derivative

of a function $f(x)$ with respect to x at point $x = x_0$ is given by

$$f'(x_0) = \frac{f(x_0 - 2h) - 8f(x_0 - h) + 8f(x_0 + h) - f(x_0 + 2h)}{12h}, \quad (6)$$

where h is a small real number that is taken to be equal to 0.05 in our calculations. The five-point formula introduces an error of $O(h^4)$ which is equal to 6.25×10^{-6} in our case.

III. WTT IN PRESENCE OF LINEAR ENVIRONMENT

In this section, we work with linear environment and consider the parameter space which allows the WTT to produce amplification. The temperature of the middle environment is taken to be in between that of the left and right environments. We consider the initial state of the system comprising the three qubits to be $|000\rangle\langle000|$, where $|0\rangle$ denotes the eigenstate of Pauli- z with eigenvalue +1. The initial state of the environment X is considered to be the thermal state, given by

$$\rho_{env}^X = \frac{e^{\hbar\Delta\beta_X\sigma_z^{(X),env}}}{\text{Tr}(e^{\hbar\Delta\beta_X\sigma_z^{(X),env}})}, \quad (7)$$

where $\beta_X = 1/(k_B T_X)$ is the inverse temperature of the environment X in units of energy $^{-1}$, for $X \in \{L, M, R\}$.

We have defined time as $t \tilde{t}$ where t is a dimensionless quantity whose magnitude denotes the magnitude of time, and \tilde{t} has the dimension of time with magnitude equal to 1. Similarly, temperature is defined as $T \tilde{T}$ where T is dimensionless quantity denoting the magnitude of temperature, and \tilde{T} has the dimension of temperature with magnitude equal to 1. \tilde{t} and \tilde{T} are related by the relation

$$\tilde{T} = \frac{\hbar}{k_B \tilde{t}},$$

where k_B denotes the Boltzmann constant and $\hbar = h/2\pi$, with h being the Planck's constant.

The initial state of the system is considered to be $|000\rangle\langle000|$, which is the ground state of the system Hamiltonian, H_{sys} . As we begin with the ground state of the system, it is expected that, during initial time evolution, heat will flow from the environment to the system. The sign convention adhered to in our work is that a positive heat current implies a flow of current from the system to the environment. This is what we numerically observe as well. The currents are initially negative at a small timescale $\sim 1\tilde{t}$. Further, since our system is not in a steady state, the relation of $J_L + J_R + J_M = 0$ is not satisfied, and hence $\alpha_R + \alpha_L + 1 = 0$ is not valid here.

The parameter range in which we perform the analyses is $T_L = 4\tilde{T}$, $T_R = 10\tilde{T}$, $\Delta = 3\tilde{t}^{-1}$, $g = 4\tilde{t}^{-1}$, the time of interaction of the system-qubit with the environment-qutrit is $\delta t = 0.5\tilde{t}$, and the time at which amplification is measured is $t = 1\tilde{t}$, unless specified. In Fig. 2, we demonstrate

the behavior the derivatives of heat currents with respect to temperature, while operating within this particular parameter regime. Fig. 2-(a) shows that, $\partial J_M/\partial T_M$, the temperature derivative of the local current of middle qubit, is smaller than that of those corresponding to other qubits, within a temperature range, $4\tilde{T}$ to $10\tilde{T}$.

This enables us to obtain amplification within a sufficiently large temperature range for the middle environment. It is to be noted that we have chosen our parameter regime where the coupling strength between the environment and the working substance is comparable to the coupling strength between the sub-parts of the working substance. We see in panel Fig. 2-(a) that since $\partial J_M/\partial T_M$ is much smaller than the other two current derivatives in this parameter space, we get a good amplification. We also note that there exists a parameter region where $\partial J_M/\partial T_M = 0$. Here the amplification is undefined. In panel (b) of Fig. 2, we have shown the variation of $\partial J_M/\partial T_M$ with T_M for different values of system-environment coupling g .

In the succeeding subsection, we study the amplification of the heat currents flowing into the the left and right qubits in presence of local environments connected to each of the qubits separately. In subsection III B, we analyze the thermal transistor effects with less than three local environments connected to three system qubits.

A. Amplification with three local environments

In this section, we consider the scenario where the system comprises three qubits, and each qubit is connected with a local environment that pertains to the collisional model composed of periodically interacting qutrits.

1. Dependence of amplification on the system-environment interaction

The performance of a WTT depends on how efficiently it can amplify the heat currents at the left and right terminals, while being modulated by the temperature of the middle terminal. Here we analyze how the amplification at the left and right terminals vary with temperature of the middle qubit by perturbatively varying the interaction strength between the working substance and environment.

Figure 3 illustrates the dynamical amplification factor at the left terminal, α_L , as a function of the middle bath's temperature, T_M , for different perturbative variations in the system-environment interaction strength, g . In this regard, we find that for a given interaction strength, the magnitude of amplification first increases until a certain value of T_M . Let us refer to this value as $T_M^{critical}$. At this particular temperature, $T_M^{critical}$, the dynamical amplification factor α_L , diverges. The divergence occurs as a result of $\partial J_M/\partial T_M$ approaching zero, indicating a point of vanishing sensitivity of the current to changes in the temperature of the middle bath. This feature is depicted in Fig. 2-(b), where the derivative of the current with respect to T_M is shown to diminish around $T_M^{critical}$. It is also observed that, at this point of discontinuity,

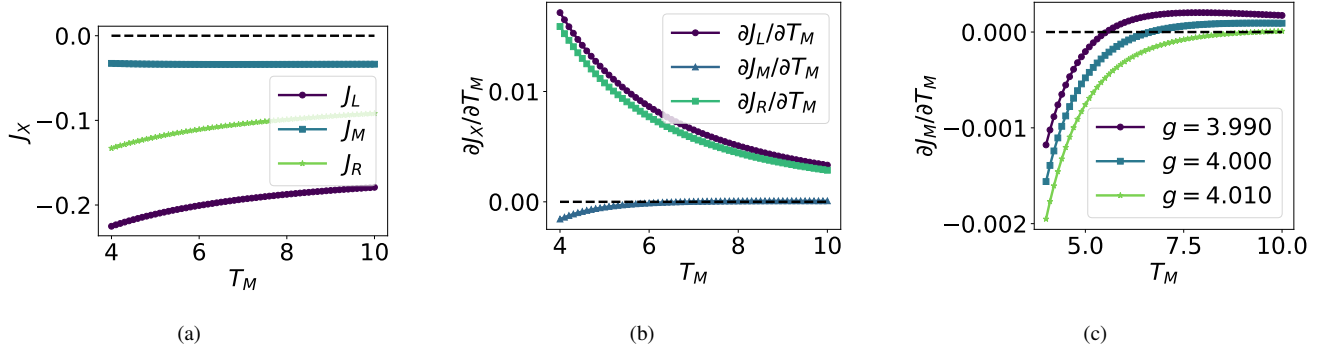


Figure 2. (a) Variation of heat currents at time $= 1 \tilde{t}$ (b) Variation of $\partial J_X/\partial T_M$ with T_M , for $X \in \{L, M, R\}$, is depicted. Values of $\partial J_M/\partial T_M$ are much smaller than the other two, and becomes equal to zero at a particular value of T_M which is equal to 6.65 in units of \tilde{T} when $g = 4$. (c) Variation of $\partial J_M/\partial T_M$ with change in the coupling constant between the qubit and the environment is demonstrated. We see that, for every value of g , the quantity $\partial J_M/\partial T_M$ becomes zero at some value of $T_M = T_M^{critical}$, which makes the amplification factor undefined. This value of $T_M^{critical}$ increases as we increases the value of g . The black dotted line is for $\partial J_M/\partial T_M = 0$. The horizontal axis has dimension \tilde{T} while the vertical axis when multiplied by \hbar/\tilde{T} will have the dimension of ratio of rate of change of energy with temperature.

the dynamical amplification factor, α_L , switches its sign from negative to positive. Towards the right of $T_M^{critical}$, i.e. where $T_M > T_M^{critical}$, the magnitude of amplification decreases and saturates to a value which is greater than one. This illustrates that transistor effect is also present for relatively higher values of T_M . The value of $T_M^{critical}$ increases with the increase of system environment interaction strength. This feature can also be understood from Fig. 2-(b), where the value of T_M for which the $\partial J_M/\partial T_M$ curve cuts the abscissa increases with increasing interaction strength. Furthermore, we show that, in the region $T_M < T_M^{critical}$, a lower interaction strength results in a higher magnitude of amplification being obtained for a particular value of T_M , whereas this trend is reversed in the $T_M > T_M^{critical}$ region, where a higher interaction strength results in higher amplification. The behavior of α_R with respect to T_M is not shown because its behavior is identical to that of α_L , and this occurs due to the symmetry between the left and right terminals of the setup.

In Fig. 2(a), we have now added a curve where the heat current flowing through the X^{th} qubit, J_X , is plotted along the vertical axis, as a function of the middle-bath temperature, T_M along the horizontal axis. Here we see that compared to the variation in J_L and J_R , the quantity J_M varies very slowly with respect to T_M . This feature is also evident from Fig. 2(b), where we see that the quantity, $\frac{\partial J_M}{\partial T_M}$, is much smaller than $\frac{\partial J_L}{\partial T_M}$ and $\frac{\partial J_R}{\partial T_M}$. Therefore, the denominator of the dynamical amplification factor becomes significantly higher than its numerator, resulting in an appreciable amplification in the parameter regime in which we work. Let us now qualitatively interpret the behavior of the amplification factor, α_L , as given in Fig. 3, by looking at the heat-current derivatives given in Figs. 2(b) and 2(c). From Fig. 2(c), we see that in the temperature regime, $T_M < T_M^{critical}$, the quantity, $\frac{\partial J_M}{\partial T_M} < 0$. Then it gradually increases to $T_M = T_M^{critical}$, where $\frac{\partial J_M}{\partial T_M} = 0$ and in the regime $T_M > T_M^{critical}$, the quantity, $\frac{\partial J_M}{\partial T_M} > 0$. Fur-

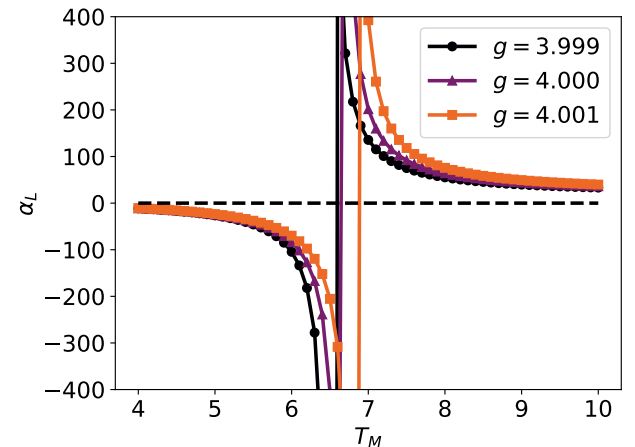


Figure 3. Variation of the dynamical amplification factor, α_L , along the vertical axis, versus the temperature of the middle bath, T_M , along the horizontal axis, for different values of system-bath interaction strength, g . We observe that there is a discontinuity in the value of α_L with respect to T_M , and an increase in the interaction strength increases and decreases the amplification to the right and left of the discontinuity respectively. The black dotted line signifies zero amplification. The quantity, α_L , is dimensionless, while T_M is in units of \tilde{T} .

ther, from Fig. 2(b) we observe that the quantity, $\frac{\partial J_L}{\partial T_M} > 0$, $\forall T_M$. Therefore, for small values of T_M , the value of $\frac{\partial J_L}{\partial T_M}$ is positive and $\frac{\partial J_M}{\partial T_M}$ is negative, which causes negative amplification. At $T_M = T_M^{critical}$, the quantity, $\frac{\partial J_M}{\partial T_M} = 0$, which causes the amplification factor, α_L , to diverge at the critical value of $T_M = T_M^{critical}$. Finally, for values of temperatures of the middle bath, $T_M > T_M^{critical}$, both $\frac{\partial J_M}{\partial T_M}$ and $\frac{\partial J_L}{\partial T_M}$ are positive, which results in positive amplification.

2. Variation of amplification with time

In this section, we analyze the variation of dynamical amplification factor of a WTT as a function of time for a given value of system-environment coupling and a fixed temperature of the environment connected to the middle qubit. We find that the variation of the dynamical amplification factor with time becomes periodic after the occurrence of a certain number of interactions between the working substance and the environment. After a finite number of interactions, we find that the amplification shoots up and falls down periodically, as shown in Fig. 4. The curve obtained by joining the maxima of each jump, corresponding to a single round of system-environment interaction, is monotonically decreasing, which depicts Markovian behavior. However a non-monotonicity is observed in the actual behavior of amplification versus time, which owes its origin to the non-Markovianity induced in the system during the periodic interaction of the bath with the working substance. This non-monotonicity in the behavior of the amplification is because of the back-flow of information from the bath to the working substance, which occurs due to the non-Markovianity induced in the system during the periodic interaction of the bath with the working substance.

The jumps occur periodically with periodicity $0.5\tilde{t}$, which is the time of interaction between each qutrit of the environment and the working substance. As a qutrit pertaining to the environment arrives to interact with a system-qubit, the amplification remains small for a short time initially and then rises abruptly to a higher value. The maximum value corresponding to each jump is reached when the qutrit has stopped interacting with a qubit of the WTT. Following this, the amplification drops as the environment-qutrit moves away from the system-qubit. Then another qutrit arrives to interact with the qubit and the entire process is repeated. Here it is interesting to note that, in the time range in which we work, the number of peaks in the amplification versus time curve, as given in Fig. 4, is sufficient large. It basically implies a wide working region of the WTT in that particular range of time.

In order to understand why there is a peak in the amplification versus time plot at $t = 1\tilde{t}$, we carried out a perturbative analysis of how the amplification factor behaves around time $t = 1$ within the relevant parameter regime. This revealed some interesting features specific to the Hamiltonian considered in our work. In particular, by varying the coupling strength between each qubit and its respective bath, we observed the following. For coupling strengths slightly below $g = 4$, the amplification is small and positive, whereas for coupling strengths slightly above $g = 4$, it becomes small and negative. The magnitude of the amplification exhibits a sharp peak at $g = 4$, where we observe a pronounced amplification, as illustrated in Fig. 5. This behavior is an intrinsic feature of the Hamiltonian model in the chosen parameter regime.

B. Amplification with less than three local environments

In this section, we consider the scenario where the system comprises three or less qubits, and the number of environments

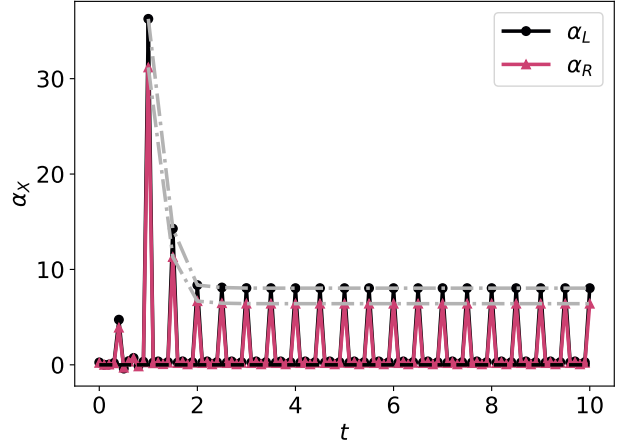


Figure 4. Variation of the dynamical amplification factor, α_X , with time, t , at $T_M = 10$. Here $X \in L, R$ where L and R denote left and right qubits respectively. We find that the variation becomes periodic after certain number of interactions have happened between the working substance and the environment. The dotted black line signifies amplification equal to zero. The vertical axis is dimensionless and the horizontal axis is in units of \tilde{t} .

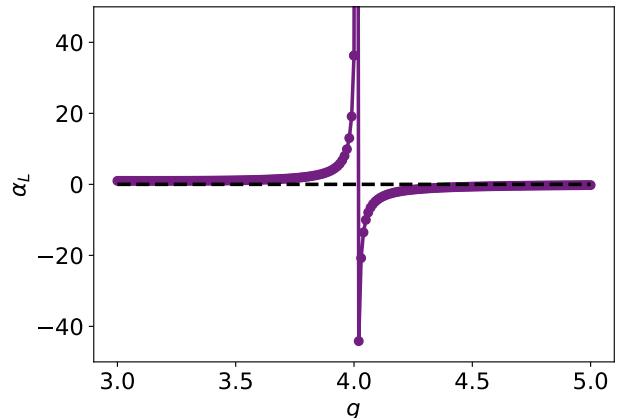


Figure 5. Variation of α_L on the vertical axis as the coupling strength g (on the horizontal axis) between the qubit and the environment is varied at $t = 1\tilde{t}$. We observe that when the coupling strength $g < 4$, the amplification is small and positive, and when $g > 4$, it is small and negative. A sharp peak in amplification occurs around $g = 4$, indicating a significant enhancement at this point.

ments interacting with the system are less than three.

1. WTTs with three qubits and two environments

To understand the role of the three environments further, we consider the case when we remove one of these environments. We have considered the middle environment, which is the modulating one, to be always present, and we remove either of the left or right environments. The temperatures of

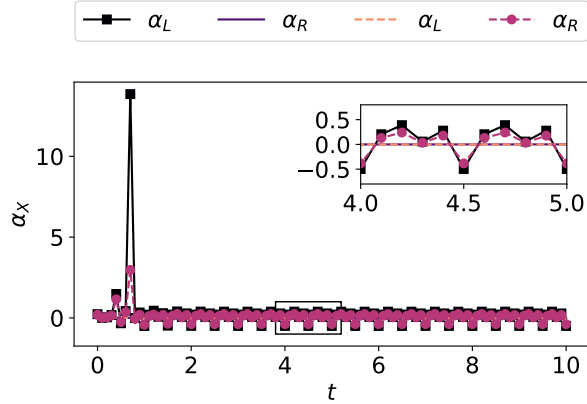


Figure 6. Variation of dynamical amplification factor with time when one of the environments is removed. The solid lines are for the system when the right environment is removed while the dotted lines are for the system when the left environment is removed. The inset shows the variation of amplification in the highlighted portion of the main graph. The vertical axis is dimensionless and the horizontal axis is in units of \tilde{t} .

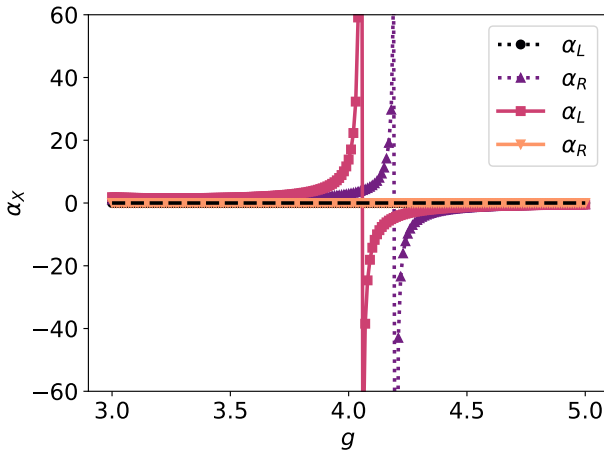


Figure 7. Variation of dynamical amplification factor with coupling strength g when one of the environments is removed. The solid lines are for the system when the right environment is removed while the dotted lines are for the system when the left environment is removed

the three environments considered for the analysis in this subsection are given by $T_L = 4\tilde{T}$, $T_M = 8\tilde{T}$, $T_R = 10\tilde{T}$.

We first remove the environment connected to the right qubit such that the right qubit only interacts with the two other qubits of the working substance to which it is coupled. We then analyze the variation of the dynamical amplification factor corresponding to the left qubit as a function of time as shown in Fig. 6. The black and purple solid curves depict α_L and α_R in this scenario respectively. We find that $\alpha_R = \partial J_R / \partial J_M$ becomes zero while α_L takes finite values

as time is varied. The value of α_R being equal to zero possibly implies that the change in current happens majorly due to the current flowing into the environments rather than into the other qubits. Since we have removed the right environment, there is no current flowing from the right qubit to the environment, and only the other two qubits are responsible for the current which remains almost zero and remains constant with respect to a change in T_M . The global maximum of α_L is attained at $0.7\tilde{t}$ seconds with the maximum value being 13.85.

The red dotted curve shows the amplification for the right qubit when the left qubit is disconnected from its environment. On the other hand, the orange dotted curve shows the amplification for left qubit which is disconnected to the environment. The behavior of amplification, α_L , versus time is qualitatively similar to the case of α_R , but with a diminished value in the amplification factor. We find that α_R reaches maximum at the end of interaction between the system and the environment. This feature is similar to what we had obtained in the case of three environments attached to the working substance in Fig. 4, with the period of each jump being the same as before, i.e. equal to the interaction time, but the maximum value being much lower in this case. We find that the values of the dynamical amplification factor are greater than 1 and a transistor effect is seen, although the amplification is not very large. The global maximum of α_R in this case is reached at $0.7\tilde{t}$ seconds with the maximum value being 2.97.

Therefore, when the environment connected to the right qubit is removed, the value of α_L follows the same qualitative trend as that of α_R when the left bath is removed. But the amplification values are slightly higher in the first case of removing the right bath. The global maxima is reached at the same value of time but is higher and reaches a value of 13.84. The disparity between the two cases is because of the two baths having unequal temperatures which affect the amplification in each of the cases.

The height of the peak of α_R and α_L in Fig. 6 at time $t = 0.7\tilde{t}$ can be explained by analyzing the variation of α with the coupling strength g as shown in Fig. 7. We see that in the case where right environment is removed (corresponding to solid pink and orange lines), the amplification is very small and monotonously increases until it reaches its peak at $g = 4.05$ and then suddenly becomes negative. After which the amplitude of the amplification keeps on decreasing. A similar trend is seen when the left environment is removed (corresponding to the dotted black and blue lines). In this case, the peak is reached at a slightly higher g value of $g = 4.2$ but the trend remains similar to that of the case when right environment was removed.

C. Symmetric versus asymmetric coupling between working-substance qubits

In the preceding subsections, we considered the case where there was no coupling between the left and right qubits of the working subsystem, and the couplings between the

left-middle and right-middle qubits were equal, i.e

$$\begin{aligned}\omega_{ML} &= \omega_{MR} = \Delta \\ \omega_{LR} &= 0.\end{aligned}\quad (8)$$

Here we consider the following two situations. In the first case, we additionally couple the left and right qubits, and consider the coupling between the left-middle, right-middle and left-right qubits to be equal, i.e.

$$\omega_{ML} = \omega_{MR} = \omega_{LR} = \Delta. \quad (9)$$

In the second case, we consider unequal couplings between each pair of qubits, i.e,

$$\begin{aligned}\omega_{ML} &= \Delta \\ \omega_{MR} &= \Delta + \delta \\ \omega_{LR} &= \Delta - \delta,\end{aligned}\quad (10)$$

where δ is a parameter considered small compared to Δ . We refer to this case as the asymmetric case. In particular, we have taken $\delta = 0.1$ and $\Delta = 3$ as before.

We calculate the dynamical amplification factor for the left and right qubits as functions of the middle bath temperature and the evolution time, for both symmetric and asymmetric coupling scenarios, and present the results in Fig. 8. Our analysis shows that amplification persists under both types of coupling. The dependence of amplification on the middle bath temperature T_M , shown in Figs. 8 (a) and (c) corresponding to symmetric and asymmetric cases, follows a trend similar to that observed previously for the coupling strengths given in Eq. 8 (refer to Fig. 3). Specifically, the amplification is initially negative, with its magnitude increasing up to a critical temperature $T_{M,A(S)}^{\text{critical}}$, beyond which it becomes positive and subsequently decreases. The value of T_M^{critical} differs between the symmetric and asymmetric cases, with the critical temperature for symmetric case being $T_{M,S}^{\text{critical}} = 1.75$ and for the asymmetric case being $T_{M,A}^{\text{critical}} = 10.45$.

The time dependence of the amplification, shown in Figs. 8 (b) and (d), also exhibits distinct features. After $t = \tilde{t}$, the amplification becomes periodic with the same period as the interaction time, consistent with the behavior reported in Fig. 4. In both symmetric and asymmetric cases, the amplification reaches its peak at $t = 0.4\tilde{t}$.

IV. RESPONSE TO NON-LINEAR ENVIRONMENTS IN AMPLIFICATION OF WTT

Equispaced energy levels in a three-level system is a highly specific scenario and imposes strict constraints on the system, while the presence of non-linearity in systems is more probable in nature. Therefore, it is necessary to investigate the impact of non-linear environments on transistor action. Furthermore, there may arise frail perturbations in the energy levels of the environment qutrit, which generate non-linearity in the environment. In this section we analyze the dynamical

amplification factor of a WTT in presence of non-linear environment. This means that the spacings between the energy levels are no longer equal as mentioned in Sec. II.

The local Hamiltonian of the environment connected to each qubit is given by

$$H_{\text{env}} = -\hbar \begin{bmatrix} \Delta & 0 & 0 \\ 0 & \epsilon & 0 \\ 0 & 0 & -\Delta \end{bmatrix}, \quad (11)$$

where ϵ is indicative of the amount of non-linearity in the environment. The condition, $\epsilon < 0$, corresponds to the three-level system being a transmon qutrit, whose energy gaps gradually decrease as we go to higher energy levels. The condition, $\epsilon > 0$, on the other hand, corresponds to Kerr type non-linearity of the environment-qutrit, where the energy gap increases as we consider higher energy levels. The quantity, $|\epsilon|$, can be considered to the strength of non-linearity (for either transmon or Kerr) present in the environment.

The three panels of Fig. 9 depict the behavior of the dynamical amplification factor for the left qubit, α_L , as a function of the temperature of the middle environment, T_M , for different values of the non-linearity strength, $|\epsilon|$. In panel (a), the amplification for the linear case, transmon, and Kerr type environments are given by the purple, black and orange curves respectively. There is a discontinuity for all these three cases occurring at $T_M = T_M^{\text{critical}}$. The amplification, in each of the cases, increase as we increase T_M when $T_M < T_M^{\text{critical}}$. We further find that in the low temperature regime, i.e. to the left of the discontinuity, Kerr type non-linearity provides a better amplification than the linear case, while in high temperature regime, i.e. to the right of the discontinuity, transmon qutrits provide an advantage in terms of better amplification than the linear case. In Fig. 9-(b), the dynamical amplification factor is plotted for different values of strength of non-linearity, $|\epsilon|$, and for $\epsilon > 0$, i.e. in the Kerr-type regime. Similar to panel (a), a discontinuity in the behavior of amplification is observed. At low T_M limit, to the left of the discontinuity of the orange curve, corresponding to $\epsilon = 0.05$, an increase in the value of non-linearity strength increases the amplification for a fixed T_M . However, to the right of the discontinuity corresponding to the value curve corresponding to $\epsilon = 0.01$, the feature is just the opposite, i.e. as we increase the strength of non-linearity, the amplification also increases.

In Fig. 9-(c), the dynamical amplification factor is plotted for different values of $|\epsilon|$, corresponding to $\epsilon < 0$, i.e. in the transmon regime. Similar to the previous scenarios, here also a discontinuity in the behavior of amplification is noted. To the left of the discontinuity of black curve corresponding to $\epsilon = -0.01$, an increase in the value of the non-linearity strength decreases the amplification with T_M . However, to the right of the discontinuity of the orange curve corresponding to $\epsilon = -0.05$, the behavior is exactly the opposite and increasing the strength of non-linearity causes an increase in amplification.

We further consider how the variation of amplification with time gets affected when non-linearity is introduced in the system, and demonstrate the results in Fig. 10. For the transmon and Kerr type environments, we observe that the amplifica-

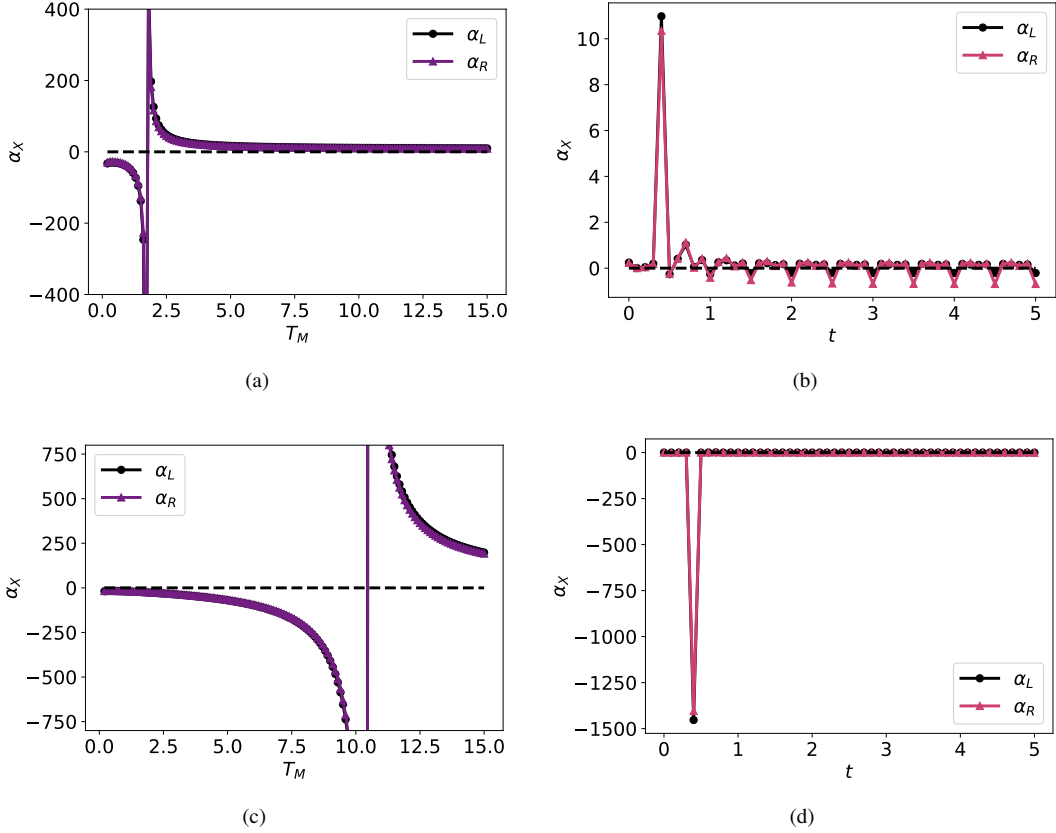


Figure 8. Variation of amplification α_X as temperature of the middle bath T_M and time t change. The top figures (a) and (b) correspond to the symmetric case where the coupling between all the qubits is Δ . The bottom figures correspond to the asymmetric coupling between the pair of qubits. The coupling between left and middle is $\Delta = 3$, between middle and right is $\Delta + 0.1 = 3.1$ and between left and right is $\Delta - 0.1 = 2.9$. (a) and (c) corresponds to time $0.4\tilde{t}$ while (b) and (d) corresponds to $T_M = 10$

tion as a function of time, follows a trend which is similar to that of the linear environment case. However, the change in amplification when we consider non-linear environments is very small ($\sim 10^{-2}$) at all points of time except at time $t = \tilde{t}$, where the amplification has significant differences, i.e. $\epsilon = -0.01$ gives an amplification of 38.98, $\epsilon = 0.01$ gives an amplification of 34.00, meanwhile linear type of environment gives an amplification of 36.27. The maximum amplification that one can attain using this setup in presence of Kerr type environments is slightly higher (38.98) than that using transmon qutrits (34.00), albeit an amplification close to the linear case is obtained in both the cases.

Next we introduce symmetric and asymmetric coupling between the qubits of the working substance along with non-linearities in the individual bath qutrits. The local Hamiltonian of the environment connected to each qubit is given by Eqn. 11 as discussed in the previous section. Meanwhile, the coupling between working-substance qubits are given by Eqns. 9 and 10 for symmetric and asymmetric coupling respectively. In particular, we have taken $\delta = 0.1$. The numerical values of amplification α_L are plotted versus the temperature of the middle bath T_M for the symmetric and asymmetric cases in Fig. 11 (a) and (b) respectively. We

show that a critical temperature exists for both symmetric and asymmetric coupling, at which a discontinuity in amplification occurs. These critical points are denoted by $T_{M,S}^{\text{critical}}$ and $T_{M,A}^{\text{critical}}$ for symmetric and asymmetric coupling, respectively. The insets in Fig. 11 provides a magnified view of regions below and above the critical temperature. We find that in both such regions, transmon-type environment offers an enhanced amplification. This is particularly different in the previous set of coupling defined by Eq. 8 where in transmon and Kerr both showed an advantage in different regions. However, in the asymmetric coupling case, the relative advantage of transmon- and Kerr-type environments follows the same qualitative behavior as observed earlier. Specifically, in the low-temperature regime (to the left of the discontinuity, i.e. $T_M < T_{M,A}^{\text{critical}}$), Kerr-type non-linearity yields stronger amplification compared to the linear case, while in the high-temperature regime (to the right of the discontinuity, i.e. $T_M > T_{M,A}^{\text{critical}}$), transmon qutrits provide superior amplification relative to the linear case.

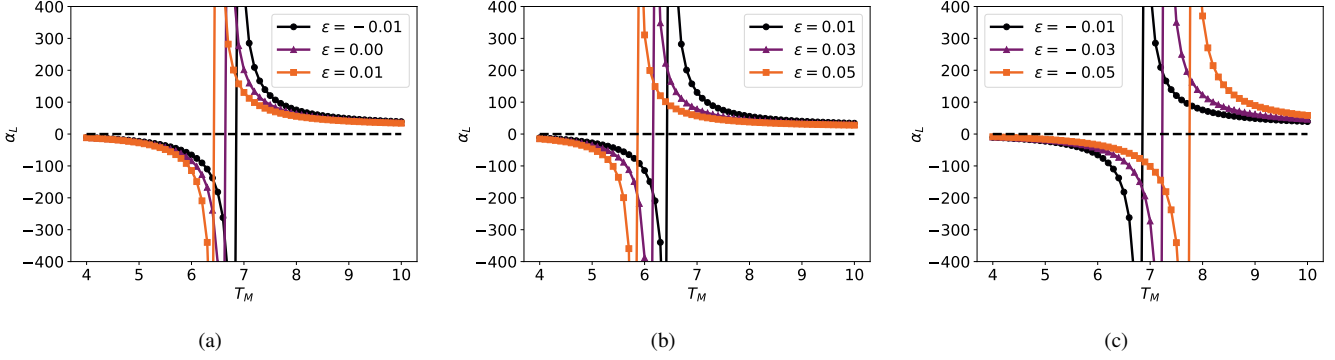


Figure 9. Variation of the dynamical amplification factor, α_L , along the vertical axis, versus the temperature of the middle bath, T_M , along the horizontal axis, for different values of non-linearity, given by ϵ . In panel (a), variation of amplification (α_L) with temperature of the middle bath, in the linear case along with the introduction of Kerr type and transmon non-linearities is given. The curves are obtained by taking time $t = 1\tilde{t}$. The variation of amplification (α_L) with temperature of the middle bath as we increase the non-linearity in the Kerr and transmon type environments at time $t = 1\tilde{t}$ are plotted in panels (b) and (c) respectively. The quantity, α_L , is dimensionless, while T_M is in units of \tilde{T} .

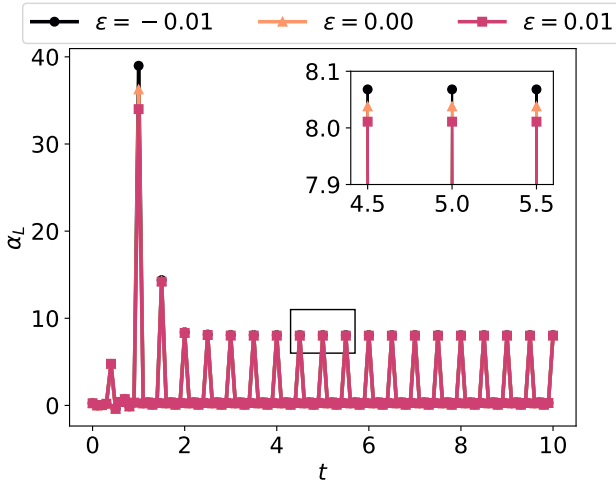


Figure 10. Variation of the dynamical amplification factor, α_L , with time, t . The inset shows the minute differences between the amplification in the case of transmon, Kerr, and linear environments in the range of time highlighted in the main graph. The vertical axis is dimensionless and the horizontal axis is in units of \tilde{t} . The given graph is at $T_M = 10$ in units of \tilde{T} .

V. QUANTIFYING NON-MARKOVIANITY

As previously mentioned, the system that we consider deals with the global unitary evolution of the system and environment, followed by discarding the environment. This is, in general, non-Markovian in nature since there are no assumptions of Markovianity. Markovianity is a special case that arises when the environment does not possess the memory of its past events, i.e. due to a memoryless environment. In our case, when the environment interacts with the system, the memory of the environment changes depending upon the interaction. So this dynamics is non-Markovian at this stage, since the environment evolves depending upon its previous memory.

However, the environment returns to its initial state periodically, i.e. there is also a loss of memory of the environment, which may potentially lead to Markovian behavior. Hence there is a tussle between memory-dependence and memory-independence of the environment in the transistor model that we have chosen. In this section, we study the memory-effects of the environment on the system, and quantify it in terms of the non-markovianity induced in the system.

Different measures have been defined to detect non-markovianity of a system undergoing a certain dynamics. We use the Breuer-Laine-Piilo (BLP) measure [78] - a faithful measure of non-markovianity - to quantify non-markovianity in our system. The trace distance, $D(\rho_1, \rho_2)$, between two states, ρ_1 and ρ_2 , is a measure of how distinguishable the two states are from each other. It is defined by

$$D(\rho_1, \rho_2) = \frac{1}{2} \text{tr} |\rho_1 - \rho_2|,$$

where the notation, $|A| = \sqrt{A^\dagger A}$, for any operator, A . The rate of change of trace distance between two states, denoted by $\sigma(t, \rho_{1,2}(0))$, is given by the following equation

$$\sigma(t, \rho_{1,2}(0)) = \frac{d}{dt} D(\rho_1(t), \rho_2(t)),$$

where t denotes time, and $\rho_{1(2)}(0)$ is the initial state of the $\rho_1(\rho_2)$. If we begin with two distinguishable states, in a quantum Markovian process, since there is loss of information from the system throughout the process, the two states will become less distinguishable with time. It implies that the value of the quantity, σ , will have negative or zero value throughout the duration of the process. But in the case of a non-Markovian quantum process, since there is back flow of information from the environment to the system, we expect that the states will become more distinguishable and hence in a non-Markovian process, σ will be positive and non-zero in a certain interval or throughout the process. The BLP measure $\mathcal{N}(\Phi)$ of non-Markovianity of a quantum process Φ is defined

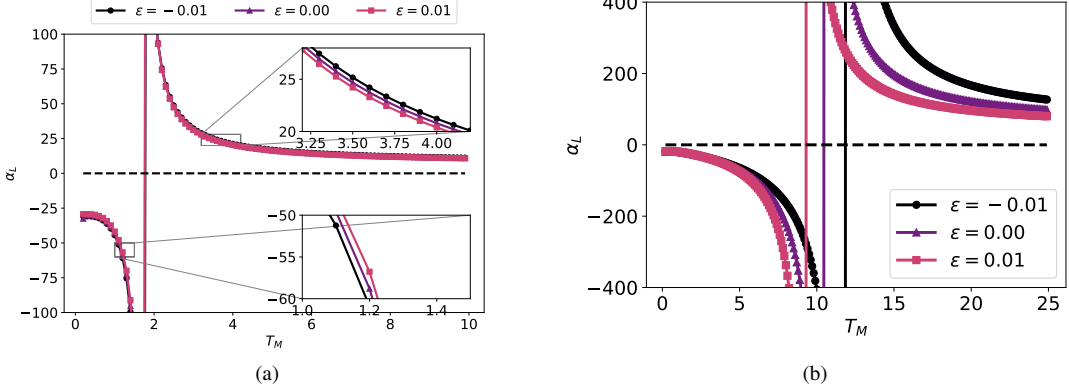


Figure 11. Variation of amplification (α_L) versus the temperature of the middle bath (T_M). The numerical analysis is done at time $t = 0.4\tilde{t}$. Panel (a) corresponds to symmetric coupling between the qubits of the working substance i.e. $\omega_{ML} = \omega_{MR} = \omega_{LR} = \Delta$. The inset in the figure shows zoomed in area with $3.2 < T_M < 4.2$. Panel (b) corresponds to asymmetric coupling between the working substance qubits i.e. $\omega_{ML} = \Delta$, $\omega_{MR} = \Delta + \delta$, $\omega_{LR} = \Delta - \delta$, where $\delta = 0.1$.

as

$$\mathcal{N}(\Phi) = \max_{\rho_{1,2}(0)} \int_{\sigma > 0} dt \sigma(t, \rho_{1,2}(0)), \quad (12)$$

where the integration is over all positive values of σ , and the maximization is over all possible input states of ρ_1 and ρ_2 .

To draw a parallel with the trends in amplification of the heat currents associated with each qubit, we consider the measure of non-markovianity for each individual qubit of the working substance. We plot the measure $\mathcal{N}(\Phi)$ for each qubit as a function of time t in Fig. 12, where the vertical axis represents $\mathcal{N}(\Phi)$ and the horizontal axis represents t . Three scenarios are considered. Panel (a) corresponds to the case where the left-middle and right-middle qubits are coupled with the interaction strength specified in Eqn. 8. Panels (b) and (c) illustrate the symmetric and asymmetric cases, respectively, with parameters chosen as described in Eqn. 9, 10 respectively. In order to do so, we optimize over the state-space comprising of single qubits. It is to note that the optimal state-pairs belong to the boundary of the state-space [79]. Further, since we work with qubits, the boundary of the state-space contains only pure states, and therefore it is sufficient to optimize over pure states only. We consider pure states of the form

$$\rho = \frac{1}{2}(\mathbb{I} + \vec{a} \cdot \vec{\sigma}), \quad (13)$$

where \vec{a} is the Bloch vector with $|\vec{a}| = 1$, and the three components of $\vec{\sigma}$ are the spin- $\frac{1}{2}$ Pauli matrices, i.e. σ_x, σ_y , and σ_z . The maximization is thus performed over the components of the Bloch vector with the constraint that the norm of the vector is equal to unity.

Noting that the system is given periodic kicks of Markovianity through successive collisions between the system and environment, it is difficult to ascertain apriori, whether non-Markovian dynamics will dominate over Markovian. In all the panels of Fig. 12, we find that at shorter timescales, there is back flow of information from the environment, and system

is non-Markovian, as indicated by non-zero value of $\mathcal{N}(\Phi)$. However, at longer timescales, viz. after time $1.5\tilde{t}$, the BLP measure $\mathcal{N}(\Phi) = 0$, implying that the system has reached a Markovian stage. This happens as the system loses memory of non-Markovian interactions at larger times. However, this Markovian feature is not reflected in the amplification (refer to Fig. 4) corresponding to the parameter set considered in Fig. 12 (a), since there are non-monotonic jumps in the amplification even after time $1.5\tilde{t}$. This is because certain quantities, like the amplification in our case, have greater memory than the measure of non-markovianity that we use here. The trend in the behavior of $\mathcal{N}(\Phi)$ is qualitatively the same for the left, middle and right qubits for all three panels, as depicted in Fig. 12 (a), Fig. 12 (b) and Fig. 12 (c).

VI. ENVIRONMENT WITH QUBITS

In this section, we aim to explore what happens when the environment consists of qubits instead of qutrits. Our primary objective is to determine whether a transistor effect persists when the working substance interacts with this type of environment.

Here we provide an analysis of the transistor action in a similar WTT model but with the environmental qutrits being replaced by qubits. In this regard, the local Hamiltonian of a single qubit of the environment gets modified to

$$H_{env} = -\hbar \Delta \sum_{i \in \{L, M, R\}} \sigma_z^{(i)}, \quad (14)$$

where $\sigma_z^{(i)}$ is the Pauli- z matrix for spin-1/2 particles. Similarly, the interaction Hamiltonian also gets modified to

$$H_{qubit-env} = -\hbar g \sum_{i \in \{L, M, R\}} \sigma_x^{(i), qubit} \sigma_x^{(i), qubit}, \quad (15)$$

where $\sigma_x^{(i), qubit}$ is the Pauli- x matrix for spin-1/2 particle, and g is the coupling constant between the system-qubit and

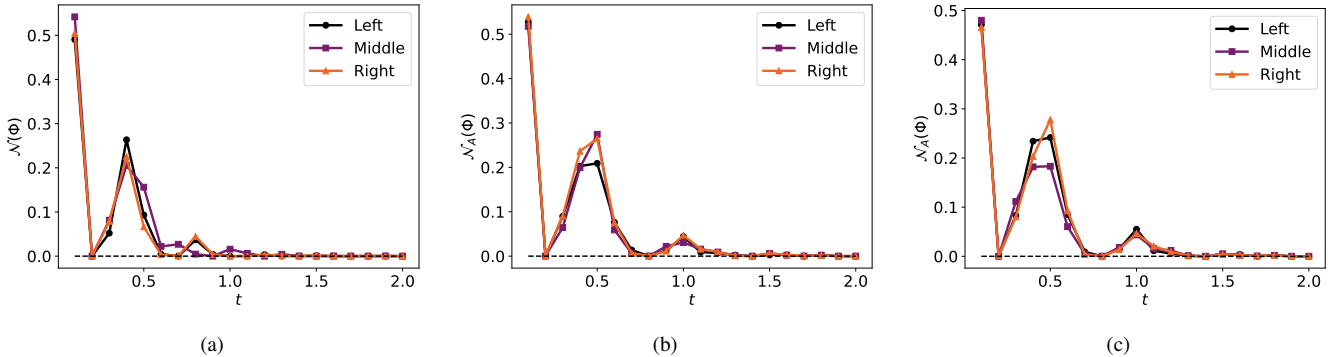


Figure 12. Plot of the BLP measure, $\mathcal{N}(\Phi)$, for each qubit of the working substance versus time, t for (a) case with $\omega_{ML} = \omega_{MR} = \Delta$, $\omega_{LR} = 0$, (b) symmetric coupling case, and (c) asymmetrical coupling case. Here the black, blue, and orange curves correspond to the amplifications for the left, middle and right qubits of working substance respectively.

the environment-qubit. The parameters considered are: $T_L = 4$, $T_R = 10$, $g = 4$, $\Delta = 3$, $T = 5$.

We have plotted the dynamic curves for the dynamical amplification factors, α_L and α_R , as functions of time t in Fig. 13 (a). The maximum values of amplification for the left and right qubits, α_L and α_R , are observed at time $9.7\tilde{t}$, with the corresponding maximum values being 37.46 and 73.67. At the same time, we have examined how the amplification associated with the left and right qubits changes as the temperature of the middle bath is varied. This behavior is illustrated in Fig. 13 (b), where it is shown that the amplifications for both qubits increase monotonically with an increase in the temperature of the middle bath. Hence, a two-level system will also be sufficient constituent of a collisional model as environment to observe transistor action.

VII. CONCLUSION

Quantum thermal transistors with Markovian baths have been rigorously studied and worked upon. Non-Markovian systems, however, are often more plausible in realistic situations. In this work, we considered a type of transistor that interacts with the environment via a collisional model consisting of a rail of qutrits, thereby deviating from Markovianity. The working substance consists of three qubits, i.e. left, right, and middle qubits. We found that such an apparatus, which we referred to as a working-substance thermal transistor, does manifest the transistor effect. The interactions between the right-middle and the left-middle qubits are considered to be equal, but there is no interaction between the left and right qubits. Such a nomenclature owes its origin to the fact that we focused on the heat currents which flow in and out of each qubit of the working substance due to the heat flow from and to the different parts of the system and environment, instead of on the currents which flow in and out of a single bath. We depicted how the figure of merit of the transistor, i.e. the amplification of the heat currents, vary with the temperature of the modulating environment, system-environment coupling and the interaction time. We have also analyzed the variation of amplification when one of the baths, that is not the modulating one, is removed.

Furthermore, we studied the effects of frail non-linearities in the environment, which are either of transmon- or Kerr-type. We found a significant amplification in each of these cases, and showed that both the type of non-linearities prove to be beneficial in different temperature regimes. In all of these cases, we also analyzed the variation of amplification with time. We found a non-monotonicity in the behavior of amplification versus time, which potentially is a manifestation of the inherent non-Markovianity in the system. We also quantified the amount of non-Markovianity by utilizing the distinguishability-based measure of Breuer, Laine and Piilo. Specifically, we found that the quantity of interest, i.e. the amplification, retains a memory of the non-Markovian interactions for a longer time than what the BLP measure itself is

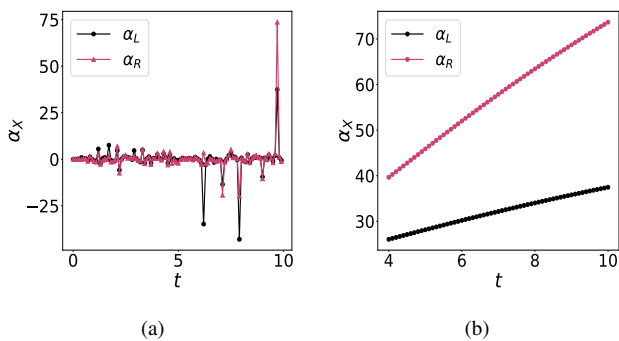


Figure 13. In panel (a) Variation of the dynamical amplification factor, α_L and α_R , with time, t . The vertical axis is dimensionless and the horizontal axis is in units of \tilde{t} . The given graph is at $T_M = 10$ in units of \tilde{T} . At the same time in panel (b) Variation of the dynamical amplification factor, α_L , along the vertical axis, versus the temperature of the middle bath, T_M , along the horizontal axis. The quantity α_L , is dimensionless, while T_M is in units of \tilde{T} . The graph is plotted at time $t = 9.7$.

able to detect. We further analyze two scenarios. In the first, the couplings among the left-middle, right-middle, and left-right qubit pairs are taken to be unequal, corresponding to the asymmetric case. In the second, all three couplings are chosen to be equal, representing the symmetric case. In both settings, we observe sufficient amplification for both the left and right qubits of the working substance. We also demonstrate a pronounced transistor effect for the left and right qubits of the working substance when the environment consists of qubits, and separately when the environment pertains non-linearities, following the same collisional model. We have also examined the non-Markovianity measure in this scenario.

ACKNOWLEDGMENTS

We acknowledge computations performed using Armadillo [80, 81] on the cluster computing facility of Harish-Chandra Research Institute (HRI), India. We acknowledge the use of **QIClib** – a modern C++ library for general purpose quantum information processing and quantum computing. DB thanks HRI for support during visits. AB acknowledges support from ‘INFOSYS scholarship for senior students’ at Harish Chandra Research Institute, India.

APPENDIX

Appendix A: Amplification with two qubits and two environments

In this subsection, we consider the case where the system comprises two qubits, left (L) and right (R), which are

connected to respective environments having temperatures T_L and T_R (in dimensions of \hat{T}) respectively. In this situation, we consider the left bath to be the modulating bath and see how a change in temperature of the left bath affects the amplification of the current in the right qubit. The dynamical amplification factor, in this case, is defined as

$$\alpha = \frac{\partial J_R}{\partial J_L} = \frac{\frac{\partial J_R}{\partial T_M}}{\frac{\partial J_L}{\partial T_M}},$$

where J_L and J_R are the heat currents flowing into the left and right qubits respectively. In this case, we observe that when the energy difference between the ground state and first excited state is the same for left and right qubit, then there is no amplification. However, when we consider unequal energy differences, there is a finite amplification in a small range of T_L . The range of T_L is from 0 to 2.488 when $\omega_L = 1$ and $\omega_R = 2$, $T_R = 4$, $g = 4$, $\Delta = 5$ and $t = 1$. In conventional classical transistors, the three components, i.e. emitter, base and collector, are all essential to observe the transistor effect, and removing any one of them suppresses this behavior. Prototypically, a two-terminal electronic device that demonstrates transistor-like effects cannot be regarded as a transistor in the classical sense. However, in the quantum mechanical domain, a two-terminal device that exhibits properties similar to a transistor can be referred to as a quantum transistor. In our work, we observe such a transistor effect in a specific regime of the left-bath temperature, T_L , when the energy gaps of the first and second excited states differ between the left and right qubits. This effect is purely quantum in nature, being absent in the corresponding classical counterparts.

[1] J. Bardeen and W. H. Brattain, “The transistor, a semiconductor triode,” *Physical Review* **74**, 230–231 (1948).

[2] J. Millman and C.C. Halkias, *Electronic Devices and Circuits*, Electrical Engineering Series (McGraw-Hill, 1967).

[3] J. Millman and C.C. Halkias, *Integrated Electronics: Analog and Digital Circuits and Systems*, Electrical Engineering Series (McGraw-Hill, 1972).

[4] R.L. Boylestad and L. Nashelsky, *Electronic Devices and Circuit Theory* (Prentice Hall, 2002).

[5] J. Bardeen and W. H. Brattain, “The transistor, a semiconductor triode,” *Phys. Rev.* **74**, 230–231 (1948).

[6] J. Bardeen and W. H. Brattain, “Physical principles involved in transistor action,” *Phys. Rev.* **75**, 1208–1225 (1949).

[7] W.F. Brinkman, D.E. Haggan, and W.W. Troutman, “A history of the invention of the transistor and where it will lead us,” *IEEE Journal of Solid-State Circuits* **32**, 1858–1865 (1997).

[8] K. Joulain, J. Drevillon, Y. Ezzahri, and J. Ordonez-Miranda, “Quantum thermal transistor,” *Phys. Rev. Lett.* **116**, 200601 (2016).

[9] R. Alicki and M. Fannes, “Entanglement boost for extractable work from ensembles of quantum batteries,” *Phys. Rev. E* **87**, 042123 (2013).

[10] F. Campaioli, F. A. Pollock, and S. Vinjanampathy, “Quantum batteries - review chapter,” *arxiv:1805.05507* (2018).

[11] S. Bhattacharjee and A. Dutta, “Quantum thermal machines and batteries,” *The European Physical Journal B* **94** (2021).

[12] J. Palao, R. Kosloff, and J. M. Gordon, “Quantum thermodynamic cooling cycle,” *Phys. Rev. E* **64**, 056130 (2001).

[13] T. Feldmann and R. Kosloff, “Quantum four-stroke heat engine: Thermodynamic observables in a model with intrinsic friction,” *Phys. Rev. E* **68**, 016101 (2003).

[14] N. Linden, S. Popescu, and P. Skrzypczyk, “How small can thermal machines be? the smallest possible refrigerator,” *Phys. Rev. Lett.* **105**, 130401 (2010).

[15] Q. Yuan, T. Wang, P. Yu, H. Zhang, and W. Zhang, H. and Ji, “A review on the electroluminescence properties of quantum-dot-lighting-emitting diodes,” *Organic Electronics* **90**, 106086 (2021).

[16] T. Werlang, M. A. Marchiori, M. F. Cornelio, and D. Valente, “Optimal rectification in the ultrastrong coupling regime,” *Phys. Rev. E* **89**, 062109 (2014).

[17] A. Chioqueta, E. Pereira, Gabriel T. Landi, and R. C. Drumond, “Rectification induced by geometry in two-dimensional quantum spin lattices,” *Phys. Rev. E* **103**, 032108 (2021).

[18] K. Poulsen, Alan C. Santos, L. B. Kristensen, and N. T. Zinner, “Entanglement-enhanced quantum rectification,” *Phys. Rev. A* **105**, 052605 (2022).

[19] B. Guo, T. Liu, and C. Yu, “Multifunctional quantum thermal device utilizing three qubits,” *Phys. Rev. E* **99**, 032112 (2019).

[20] M. T. Naseem, A. Misra, O. E. Müstecaplıoğlu, and G. Kurizki, “Minimal quantum heat manager boosted by bath spectral filtering,” *Phys. Rev. Res.* **2**, 033285 (2020).

[21] R. Ghosh, A. Ghoshal, and U. Sen, “Quantum thermal transistors: Operation characteristics in steady state versus transient regimes,” *Phys. Rev. A* **103**, 052613 (2021).

[22] A. Mandarino, K. Joulain, M. Domínguez Gómez, and B. Bellomo, “Thermal transistor effect in quantum systems,” *Phys. Rev. Appl.* **16**, 034026 (2021).

[23] Y. Huangfu, S. Qi, and J. Jing, “A multifunctional quantum thermal device: With and without inner coupling,” *Physics Letters A* **393**, 127172 (2021).

[24] Q. Ruan, W. Liu, and L. Wang, “Dynamic response of a thermal transistor to time-varying signals,” *Chinese Physics B* **33**, 056301 (2024).

[25] H. Yang and Y. Tan, “Quantum thermal transistor: a unified method from weak to strong internal coupling,” *Journal of Physics B: Atomic, Molecular and Optical Physics* **53**, 205504 (2020).

[26] B. Guo, T. Liu, and C. Yu, “Quantum thermal transistor based on qubit-qutrit coupling,” *Phys. Rev. E* **98**, 022118 (2018).

[27] N. Gupt, S. Bhattacharyya, B. Das, S. Datta, V. Mukherjee, and A. Ghosh, “Floquet quantum thermal transistor,” *Phys. Rev. E* **106**, 024110 (2022).

[28] S. Das, S. Mahunta, N. Gupt, V. Mukherjee, and A. Ghosh, “Fluctuations and optimal control in a floquet quantum thermal transistor,” .

[29] J. Yang, C. Elouard, J. Splettstoesser, B. Sothmann, R. Sánchez, and A. N. Jordan, “Thermal transistor and thermometer based on coulomb-coupled conductors,” *Phys. Rev. B* **100**, 045418 (2019).

[30] Y. Zhang, Z. Yang, X. Zhang, B. Lin, G. Lin, and J. Chen, “Coulomb-coupled quantum-dot thermal transistors,” *EPL (Europhysics Letters)* **122**, 17002 (2018).

[31] C. Wang and D. Xu, “A polaron theory of quantum thermal transistor in nonequilibrium three-level systems*,” *Chinese Physics B* **29**, 080504 (2020).

[32] B. Xiong, X. Li, S. Chao, and L. Zhou, “Quantum transistor with a double-cavity optomechanical system,” *EPL (Europhysics Letters)* **122**, 64002 (2018).

[33] G. Tang, J. Peng, and J. Wang, “Three-terminal normal-superconductor junction as thermal transistor,” *The European Physical Journal B* **92** (2019).

[34] U. N. Ekanayake, S. D. Gunapala, and M. Premaratne, “Stochastic model of noise for a quantum thermal transistor,” *Physical Review B* **108** (2023).

[35] Y. Liu, D. Yu, and C. Yu, “Common environmental effects on quantum thermal transistor,” *Entropy* **24**, 32 (2021).

[36] U. N. Ekanayake, S. D. Gunapala, and M. Premaratne, “Engineered common environmental effects on multitransistor systems,” *Phys. Rev. B* **107**, 075440 (2023).

[37] A. Mandarino, “Quantum thermal amplifiers with engineered dissipation,” *Entropy* **24** (2022).

[38] S. Su, Y. Zhang, B. Andresen, and J. Chen, “Coherence-enhanced thermal amplification for small systems,” *Physica A: Statistical Mechanics and its Applications* **569**, 125753 (2021).

[39] C. Wang, X. Chen, K. Sun, and J. Ren, “Heat amplification and negative differential thermal conductance in a strongly coupled nonequilibrium spin-boson system,” *Physical Review A* **97** (2018).

[40] H. Liu, C. Wang, L. Q. Wang, and J. Ren, “Strong system-bath coupling induces negative differential thermal conductance and heat amplification in nonequilibrium two-qubit systems,” *Physical Review E* **99** (2019).

[41] T. Wu, Y. Yang, T. Wang, X. Li, and L. Zhang, “Optimizing the performance of the thermal transistor based on negative differential thermal resistance,” *Applied Physics Letters* **124** (2024).

[42] S. Su, Y. Zhang, B. Andresen, and J. Chen, “Quantum coherence thermal transistors,” *arXiv:1811.02400* (2018).

[43] R. T. Wijesekara, S. D. Gunapala, and M. Premaratne, “Darlington pair of quantum thermal transistors,” *Physical Review B* **104** (2021).

[44] R. T. Wijesekara, S. D. Gunapala, and M. Premaratne, “Towards quantum thermal multi-transistor systems: Energy divider formalism,” *Physical Review B* **105** (2022).

[45] G. T. Craven and A. Nitzan, “Electrothermal transistor effect and cyclic electronic currents in multithermal charge transfer networks,” *Physical Review Letters* **118** (2017).

[46] A. Gubaydullin, G. Thomas, D. S. Golubev, D. Lvov, J. T. Peltonen, and J. P. Pekola, “Photonic heat transport in three terminal superconducting circuit,” *Nature Communications* **13** (2022).

[47] M. Majland, K. Sangild Christensen, and Nikolaj T. Z., “Quantum thermal transistor in superconducting circuits,” *Phys. Rev. B* **101**, 184510 (2020).

[48] J. Ordonez-Miranda, Y. Ezzahri, J. Drevillon, and K. Joulain, “Transistorlike device for heating and cooling based on the thermal hysteresis of vo_2 ,” *Phys. Rev. Appl.* **6**, 054003 (2016).

[49] H. Prod’Homme, J. Ordonez-Miranda, Y. Ezzahri, J. Drevillon, and K. Joulain, “ vo_2 -based radiative thermal transistor in the static regime,” *arXiv:1710.10332* (2017).

[50] L. Castelli, Q. Zhu, T. J. Shimokusu, and G. Wehmeyer, “A three-terminal magnetic thermal transistor,” *Nature Communications* **14** (2023).

[51] P. P. Hofer, M. Perarnau-Llobet, L. D. M. Miranda, G. Haack, R. Silva, J. B. Brask, and N. Brunner, “Markovian master equations for quantum thermal machines: local versus global approach,” *New Journal of Physics* **19**, 123037 (2017).

[52] A. Hewgill, G. De Chiara, and A. Imparato, “Quantum thermodynamically consistent local master equations,” *Physical Review Research* **3** (2021).

[53] J. Fischer and H. Breuer, “Correlated projection operator approach to non-markovian dynamics in spin baths,” *Phys. Rev. A* **76**, 052119 (2007).

[54] S. Bhattacharya, A. Misra, C. Mukhopadhyay, and A. K. Pati, “Exact master equation for a spin interacting with a spin bath: Non-markovianity and negative entropy production rate,” *Phys. Rev. A* **95**, 012122 (2017).

[55] A. Bhattacharyya, A. Ghoshal, and U. Sen, “Transient effects in quantum refrigerators with finite environments,” *Phys. Rev. A* **111**, 012209 (2025).

[56] Sukrut Mondkar, Aparajita Bhattacharyya, and Ujjwal Sen, “Quantum refrigerator embedded in spin-star environments: Scalings of temperature and refrigeration time,” *arXiv:2505.04374* (2025).

[57] E. Bäumer, M. Perarnau-Llobet, P. Kammerlander, Henrik Wilming, and R. Renner, “Imperfect Thermalizations Allow for Optimal Thermodynamic Processes,” *Quantum* **3**, 153 (2019).

[58] V. Scarani, M. Ziman, P. Štelmachovič, N. Gisin, and V. Bužek, “Thermalizing quantum machines: Dissipation and entanglement,” *Phys. Rev. Lett.* **88**, 097905 (2002).

[59] L. Bruneau, A. Joye, and M. Merkli, “Repeated interactions in open quantum systems,” *Journal of Mathematical Physics* **55**, 075204 (2014).

[60] D. Grimmer, D. Layden, Robert B. Mann, and E. Martín-Martínez, “Open dynamics under rapid repeated interaction,” *Phys. Rev. A* **94**, 032126 (2016).

[61] P. Strasberg, G. Schaller, T. Brandes, and M. Esposito, “Quantum and information thermodynamics: A unifying framework based on repeated interactions,” *Phys. Rev. X* **7**, 021003 (2017).

[62] K. Sen and U. Sen, “Noisy quantum batteries,” *arXiv:2302.07166* (2023).

[63] D. Morrone, M. A. C. Rossi, A. Smirne, and M. G. Genoni, “Charging a quantum battery in a non-markovian environment: a collisional model approach,” *Quantum Science and Technology* **8**, 035007 (2023).

[64] S. Seah, S. Nimmrichter, and V. Scarani, “Nonequilibrium dynamics with finite-time repeated interactions,” *Phys. Rev. E* **99**, 042103 (2019).

[65] M. Cattaneo, G. De Chiara, S. Maniscalco, R. Zambrini, and G. L. Giorgi, “Collision models can efficiently simulate any multipartite markovian quantum dynamics,” *Phys. Rev. Lett.* **126**, 130403 (2021).

[66] P. Strasberg, “Repeated interactions and quantum stochastic thermodynamics at strong coupling,” *Phys. Rev. Lett.* **123**, 180604 (2019).

[67] F. L. S. Rodrigues, G. De Chiara, M. Paternostro, and G. T. Landi, “Thermodynamics of weakly coherent collisional models,” *Phys. Rev. Lett.* **123**, 140601 (2019).

[68] K. Hammam, Y. Hassouni, R. Fazio, and G. Manzano, “Optimizing autonomous thermal machines powered by energetic coherence,” *New Journal of Physics* **23**, 043024 (2021).

[69] J. Koch, T. M. Yu, J. Gambetta, A. A. Houck, D. I. Schuster, J. Majer, A. Blais, M. H. Devoret, S. M. Girvin, and R. J. Schoelkopf, “Charge-insensitive qubit design derived from the cooper pair box,” *Phys. Rev. A* **76**, 042319 (2007).

[70] B.D. Josephson, “Possible new effects in superconductive tunnelling,” *Physics Letters* **1**, 251–253 (1962).

[71] T. Ray, A. Ghoshal, D. Rakshit, and U. Sen, “Optimal quantum resource generation by coupled transmons immersed in markovian baths,” *Phys. Rev. A* **108**, 052417 (2023).

[72] J. Krause, C. Dickel, E. Vaal, M. Vielmetter, J. Feng, R. Bounds, G. Catelani, J. M. Fink, and Y. Ando, “Magnetic field resilience of three-dimensional transmons with thin-film $\text{al}/\text{alo}_x/\text{Al}$ josephson junctions approaching 1 t,” *Phys. Rev. Appl.* **17**, 034032 (2022).

[73] A. Bhattacharyya, P. Dongre, and U. Sen, “Nonlinearity-assisted advantage for charger-supported open quantum batteries,” *arXiv:2410.00618* (2024).

[74] T. Ray, S. Mondal, A. Bhattacharyya, A. Ghoshal, D. Rakshit, and U. Sen, “Kerr-type nonlinear baths enhance cooling in quantum refrigerators,” *arXiv:2311.10499* (2023).

[75] V. Gorini, A. Kossakowski, and E. C. G. Sudarshan, “Completely positive dynamical semigroups of n-level systems,” *Journal of Mathematical Physics* **17**, 821–825 (1976).

[76] G. Lindblad, “On the generators of quantum dynamical semigroups,” *Communications in Mathematical Physics* **48**, 119–130 (1976).

[77] H.P. Breuer and F. Petruccione, *The Theory of Open Quantum Systems* (Oxford University Press, 2002).

[78] H. Breuer, E. Laine, and J. Piilo, “Measure for the degree of non-markovian behavior of quantum processes in open systems,” *Phys. Rev. Lett.* **103**, 210401 (2009).

[79] S. Wißmann, A. Karlsson, E. M. Laine, J. Piilo, and H. P. Breuer, “Optimal state pairs for non-markovian quantum dynamics,” *Phys. Rev. A* **86**, 062108 (2012).

[80] C. Sanderson and R. Curtin, “Armadillo: A template-based c++ library for linear algebra,” *Journal of Open Source Software* **1**, 26 (2016).

[81] C. Sanderson and R. Curtin, “A user-friendly hybrid sparse matrix class in c++,” *Mathematical Software – ICMS 2018*, , 422–430 (2018).